Nuclei Instance Segmentation in Pathology Image

Chenming Zhu

June 18, 2020

Papers:

CIA-Net: Robust Nuclei Instance Segmentation with Contour-aware Information Aggregation

(Early accepted by MICCAI 2020) Boundary-assisted Region Proposal Networks for Nucleus Segmentation

Cell R-CNN V3: A Novel Panoptic Paradigm for Instance Segmentation in Biomedical Images

Problems: Nulcei instance segmentation

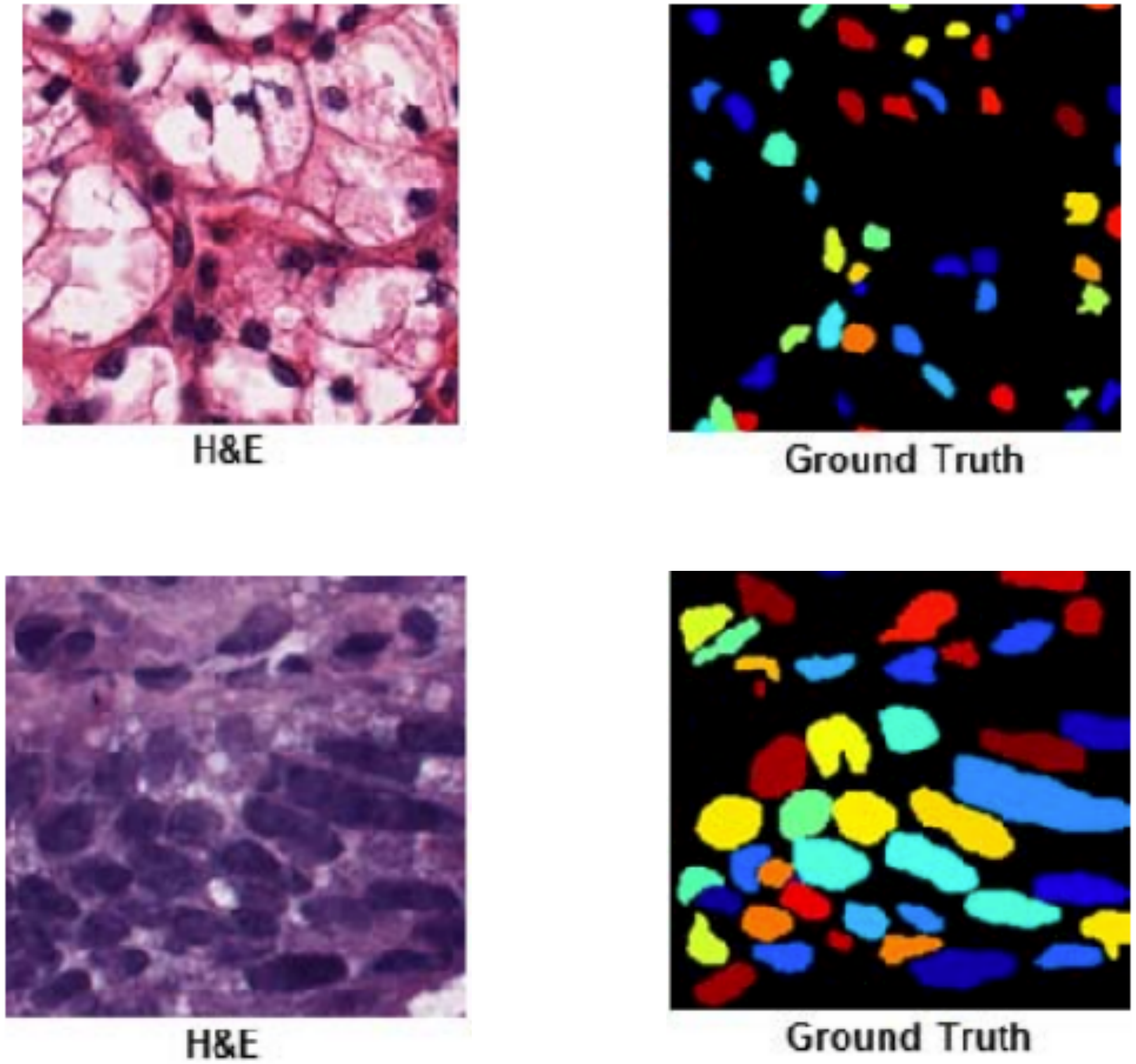

nuclei instance segmentation which not only captures location and density information but also rich morphology features, such as magnitude and the cytoplasmic ratio, is critical in tumor diagnosis and following treatment procedures

Challenges:

1. nuclei occlusions and clusters cause over/under-segmentation

over-segmentation

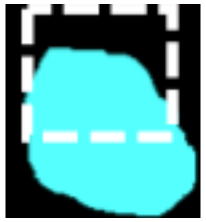

GT

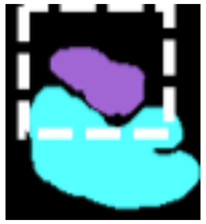

Segmented

under-segmentation

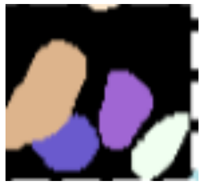

GT

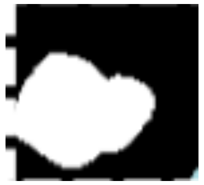

Segmented

2. the blurred border and inconsistent staining -> indistinguishable instances

3. the variability in cell appearance, magnitude, and density

Methods:

1. Traditional methods : based on thresholding and morphological operations

2. Mask R-CNN based methods:

Cell RCNN -> Cell R-CNN V2-> Cell R-CNN V3

3. U-net like methods:

DCAN -> BES-Net -> CIA-Net -> BRP-Net

CIA-Net: Robust Nuclei Instance Segmentation with Contour-aware Information Aggregation

Introduction:

Based on boundary detection to achieve instance segmentation

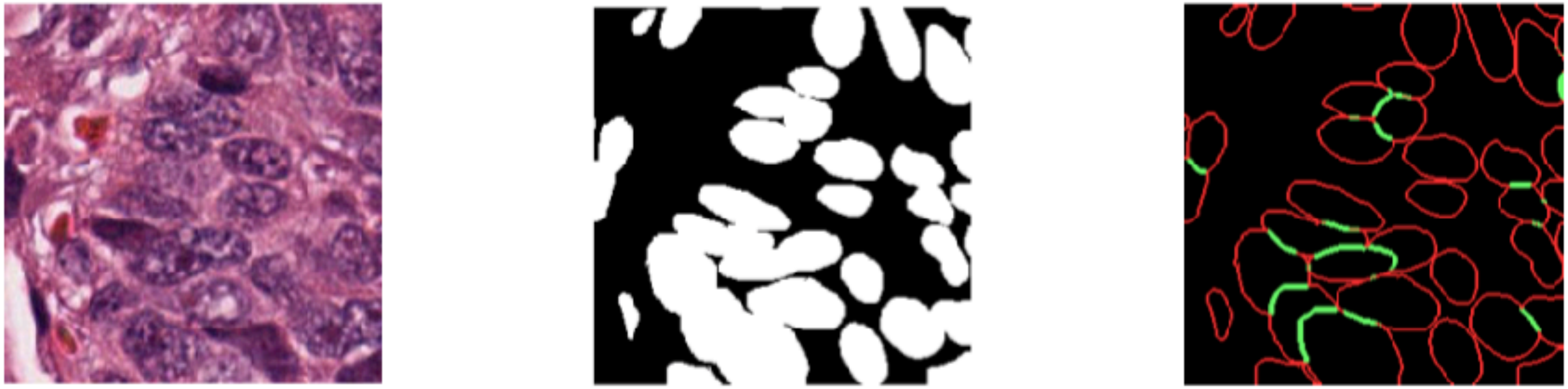

(a) (b) (c)

Model:

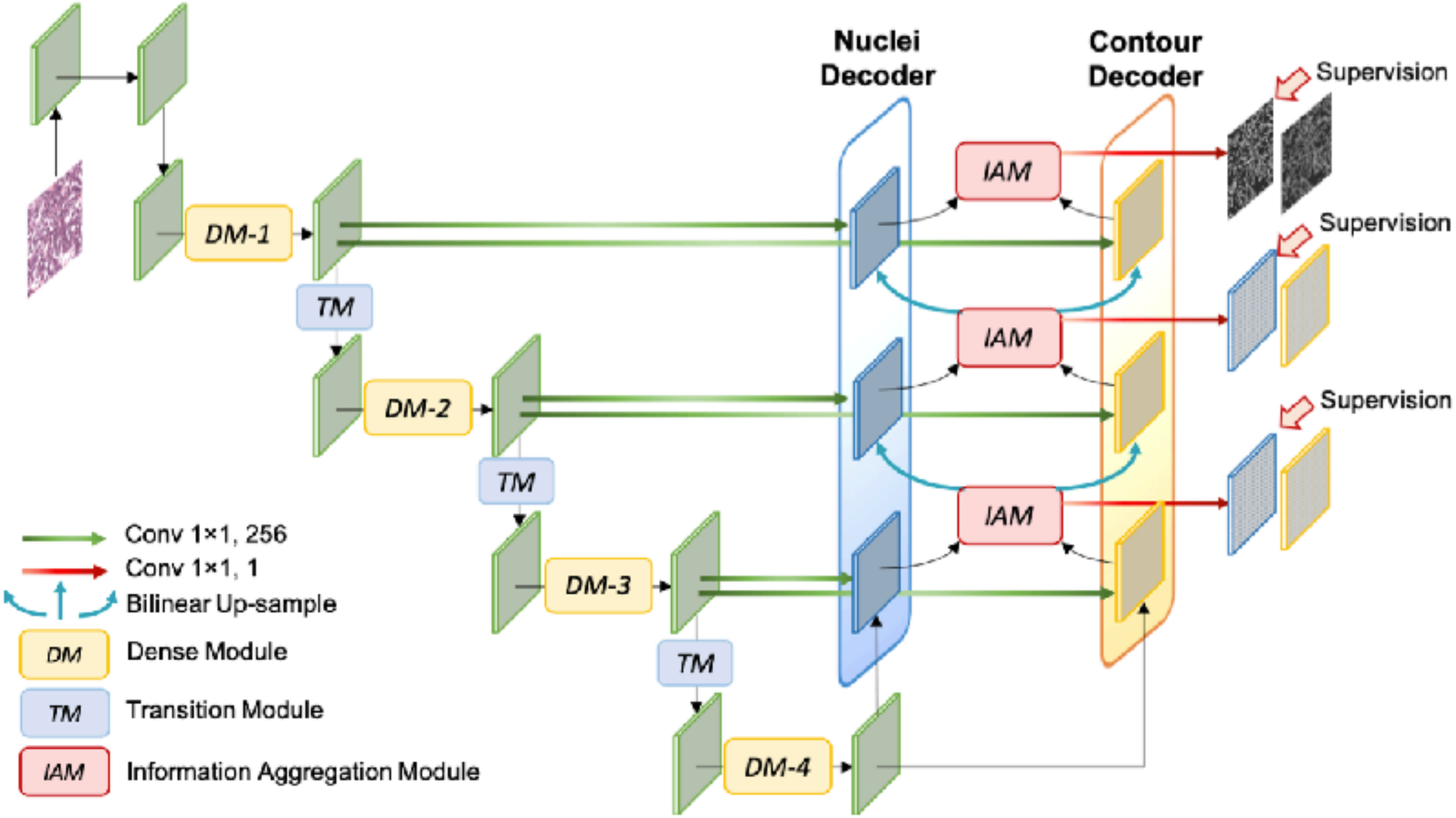

IAM + Deep Supervision

Model:

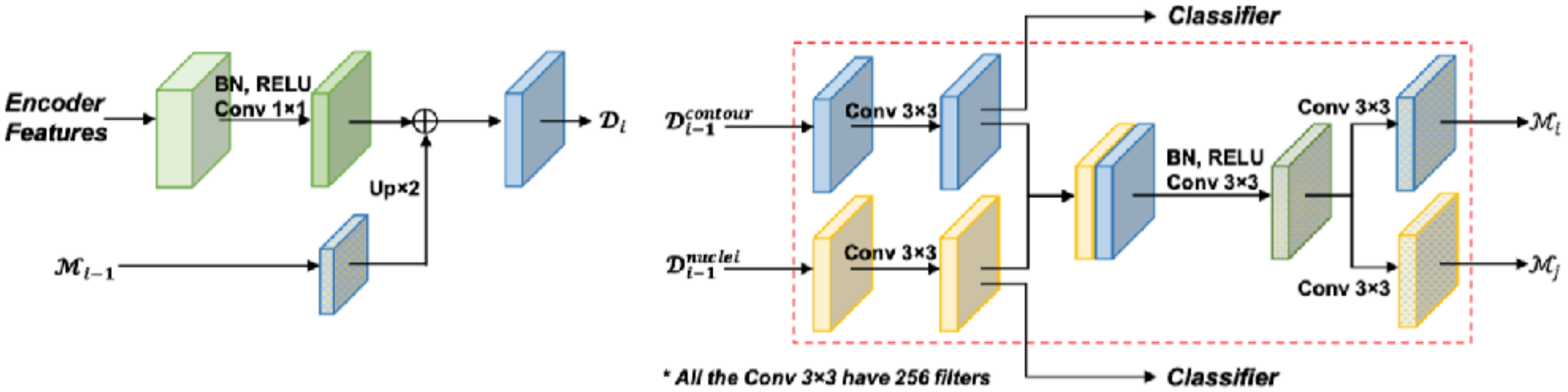

* All the Conv 3×3 have 256 filters

(a) Lateral Connected Refinement

(b) Information Aggregation Module

IAM: aggregate the task-specific features between two decoders

Smooth Truncated Loss:

blurred edge and inconsistent staining -> mislabelled objects and inaccurate boundary

$$\mathcal{L}_{ST} = \begin{cases} -\log(\gamma) + \frac{1}{2}(1 - \frac{p_t^2}{\gamma^2}), & p_t < \gamma \\ -\log(p_t), & p_t \geqslant \gamma \end{cases}$$

$$p_t = p \text{ if } t = 1 \text{ and } p_t = 1{-}p \text{ otherwise}$$

$$\mathcal{L}_{total} = \mathcal{L}_{ST} + \lambda \mathcal{L}_{Dice} + \beta \|\mathcal{W}\|_2^2,$$

Results:

Datasets:

TCGA- Kumar: 30 1000*1000 Images, 16 training images, 14 testing images（8 seen, 6 unseen)

Performance:

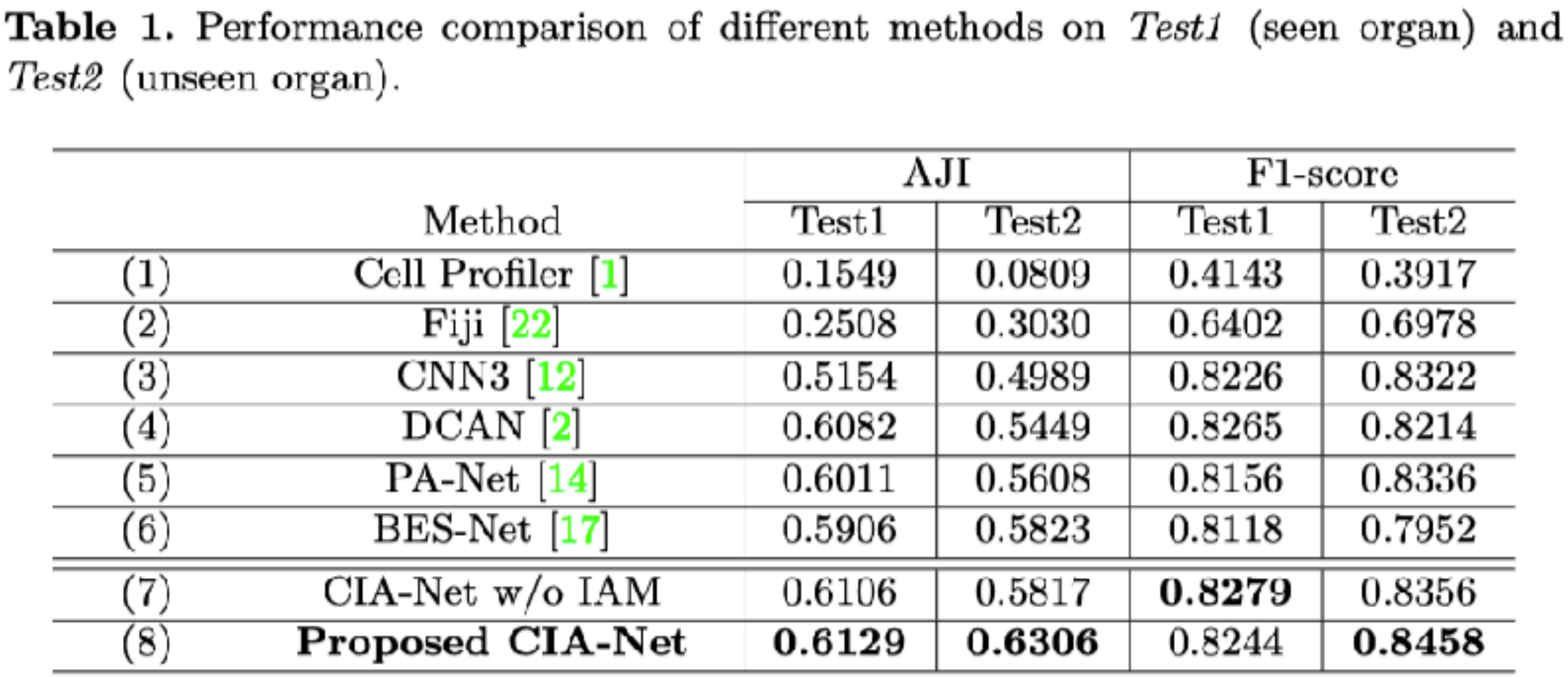

Table 1. Performance comparison of different methods on *Test1* (seen organ) and *Test2* (unseen organ).

	Method	AJI		F1-score	
		Test1	Test2	Test1	Test2
(1)	Cell Profiler [1]	0.1549	0.0809	0.4143	0.3917
(2)	Fiji [22]	0.2508	0.3030	0.6402	0.6978
(3)	CNN3 [12]	0.5154	0.4989	0.8226	0.8322
(4)	DCAN [2]	0.6082	0.5449	0.8265	0.8214
(5)	PA-Net [14]	0.6011	0.5608	0.8156	0.8336
(6)	BES-Net [17]	0.5906	0.5823	0.8118	0.7952
(7)	CIA-Net w/o IAM	0.6106	0.5817	**0.8279**	0.8356
(8)	**Proposed CIA-Net**	**0.6129**	**0.6306**	0.8244	**0.8458**

Results:

Ablations:

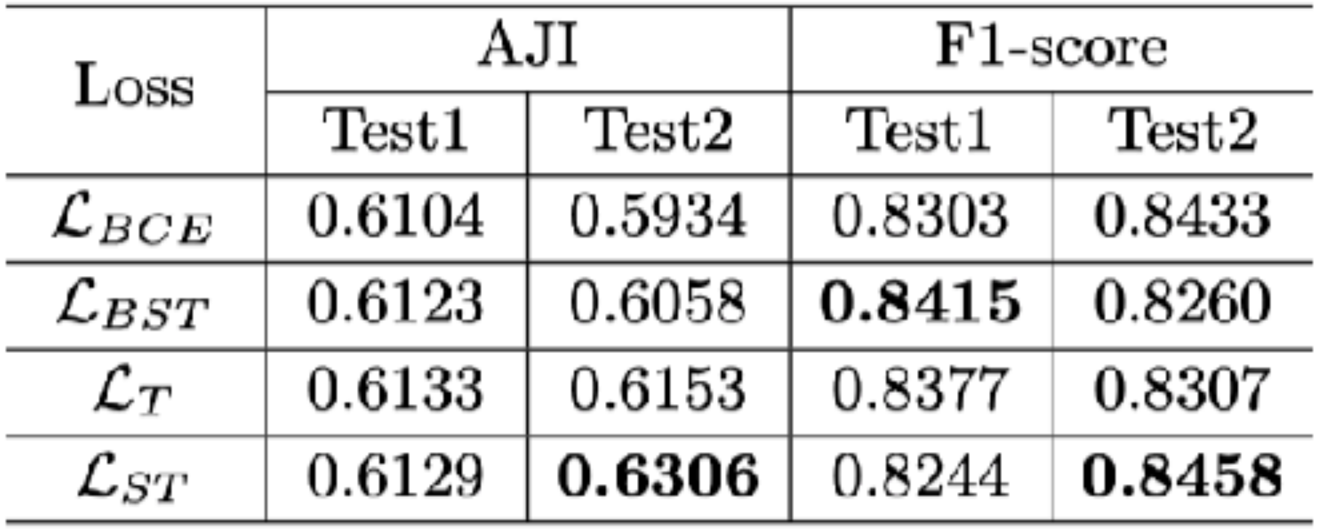

Loss	AJI		F1-score	
	Test1	Test2	Test1	Test2
$\mathcal{L}_{BCE}$	0.6104	0.5934	0.8303	0.8433
$\mathcal{L}_{BST}$	0.6123	0.6058	**0.8415**	0.8260
$\mathcal{L}_{T}$	0.6133	0.6153	0.8377	0.8307
$\mathcal{L}_{ST}$	0.6129	**0.6306**	0.8244	**0.8458**

Table 2. Comparison of proposed CIA-Net with different loss functions.

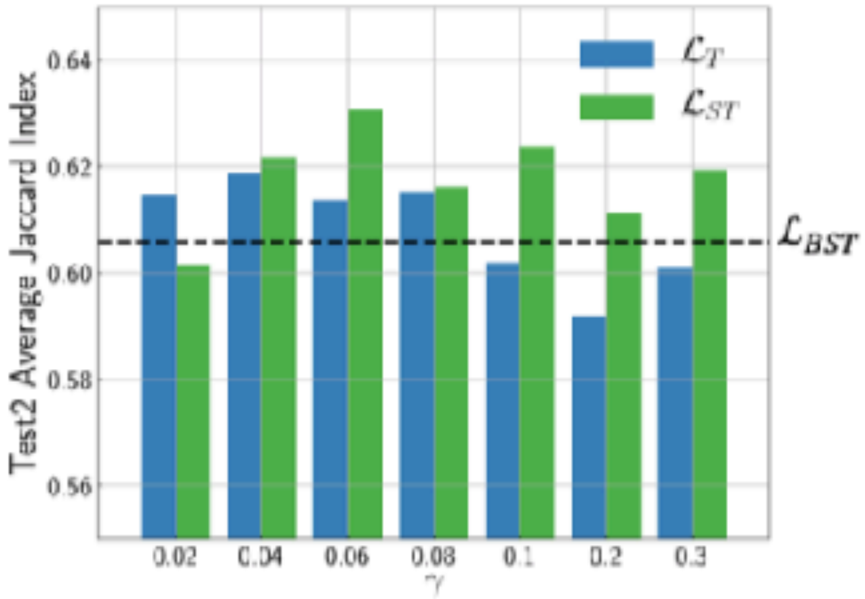

Fig. 4. Results of varying γ for $\mathcal{L}_T$ and $\mathcal{L}_{ST}$ on *Test2*.

(Early accepted by MICCAI 2020) Boundary-assisted Region Proposal Networks for Nucleus Segmentation

Shengcong Chen 1[0000−0002−8019−9675] , Changxing Ding 1[0000−0001−7232−3181] ,
and Dacheng Tao 2[0000−0001−7225−5449]

1.School of Electronic and Information Engineering, South China University of Technology,
Guangzhou 510641, China c.shengcong@mail.scut.edu.cn, chxding@scut.edu.cn UBTECH
2.Sydney AI Centre, School of Computer Science, Faculty of Engineering, The University of
Sydney, Darlington, NSW 2008, Australia

Introductions:

Two stage: 1/ use boundary detection-based scheme to obtain instance proposals

2/ refines the segmentation for each proposals

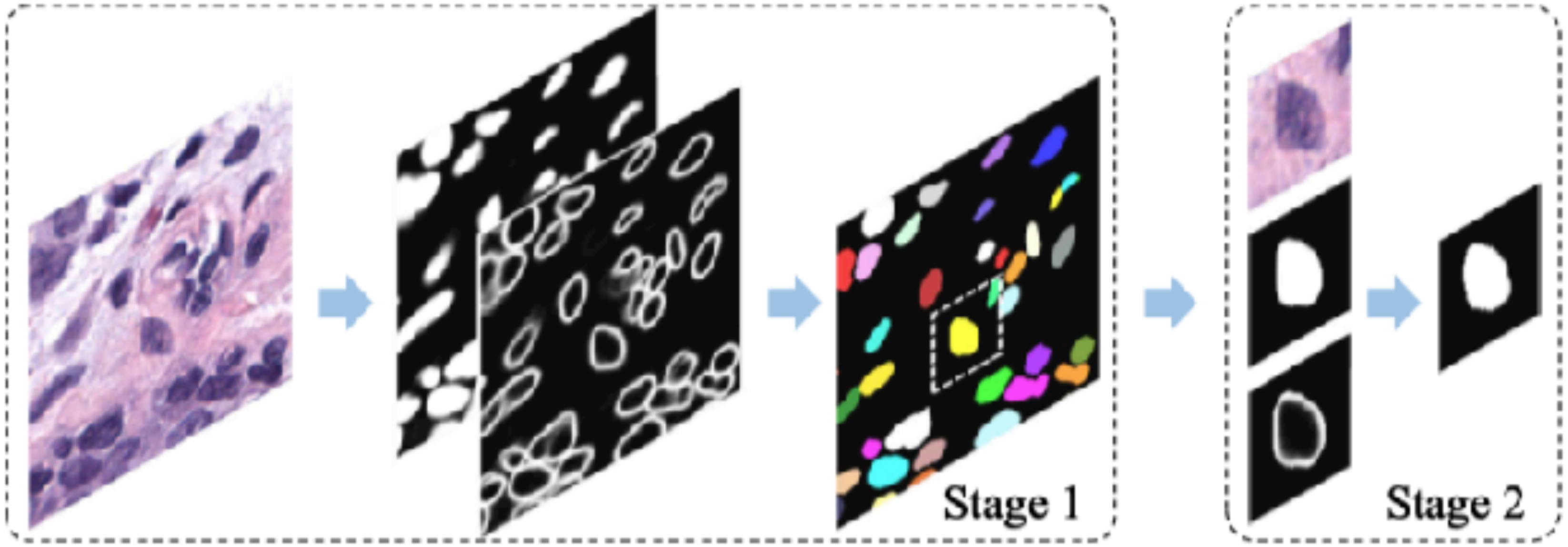

Fig. 2. Overview of BRP-Net. BRP-Net comprises two stages: one stage to obtain instance proposals and another for proposal-wise segmentation.

Model:

TAFE:

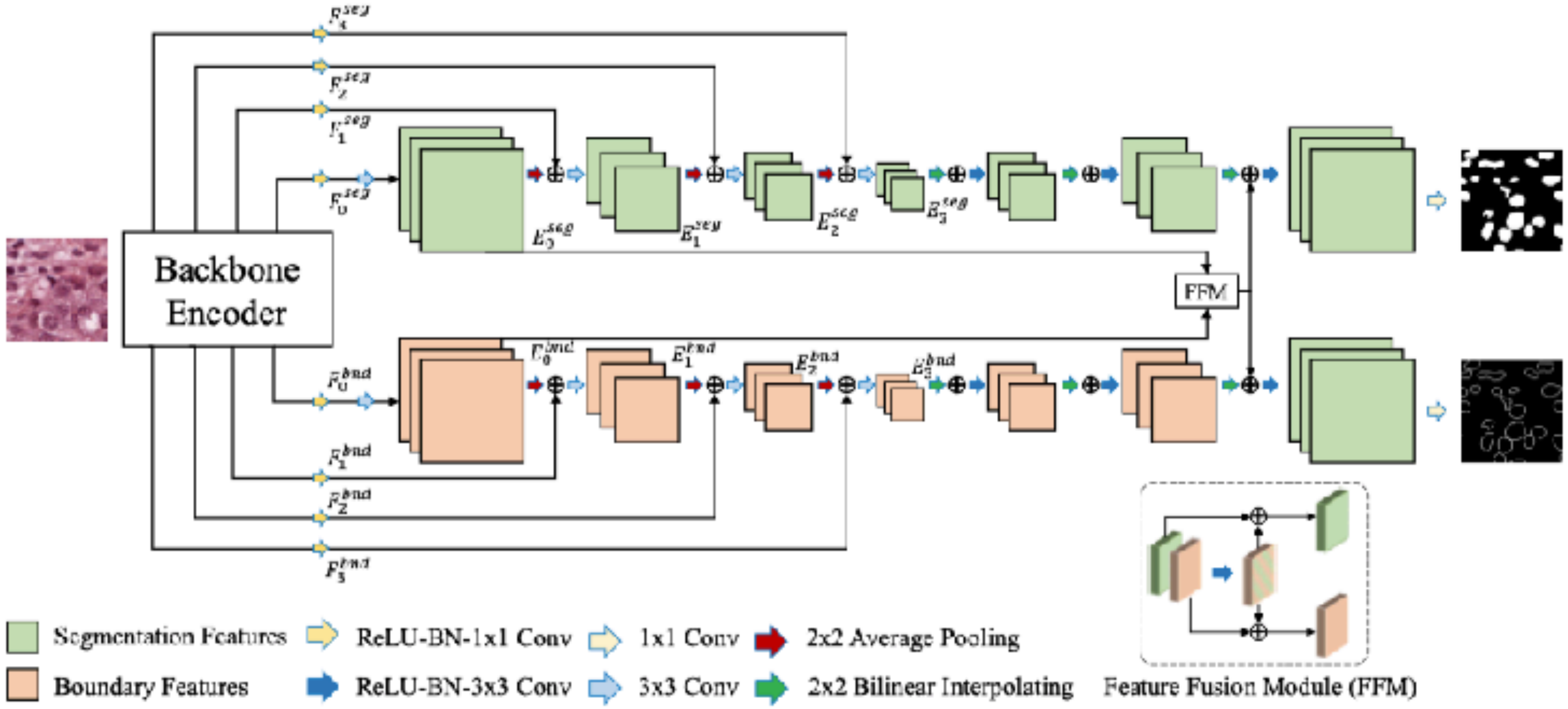

Fig. 3. Architecture details of TAFE. The number of channels in F_i is set to 256 consistently. Feature maps produced by both encoders are fused in FFMs to make use of their correlation. For simplicity, only one FFM is shown and the other two FFMs are ignored in this figure. (Best viewed in color).

Model:

Proposal-wise Segmentation:

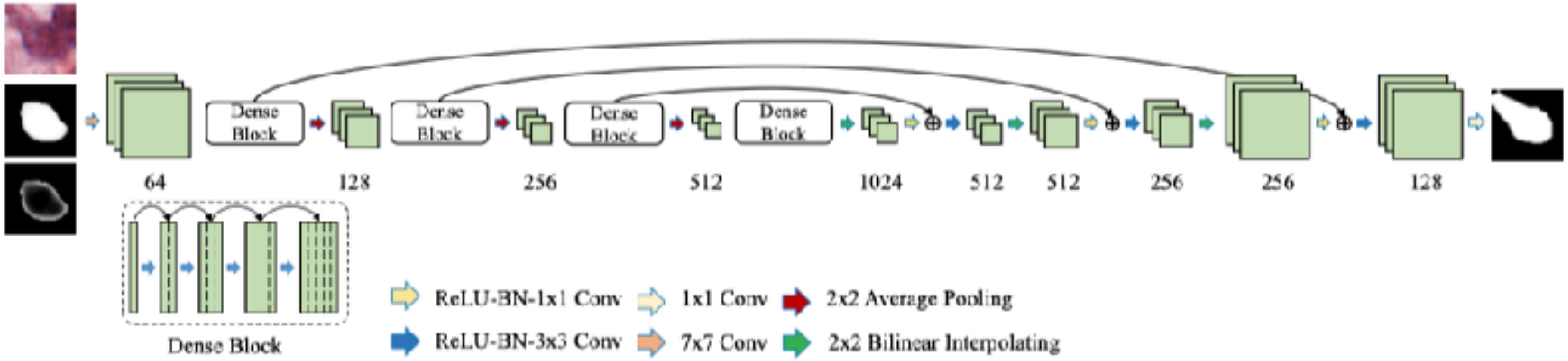

Fig. 4. The two networks in the proposal-wise segmentation stage adopt the same architecture. Each layer in the network includes one dense block that consists of four 3×3 convolutional layers. Growth rates of the four dense blocks are set to 16, 32, 64, and 128, respectively. The number below each group of feature maps denotes the number of channels. (Best viewed in color).

Results:

Datasets: TCGA-Kumar

Ablations:

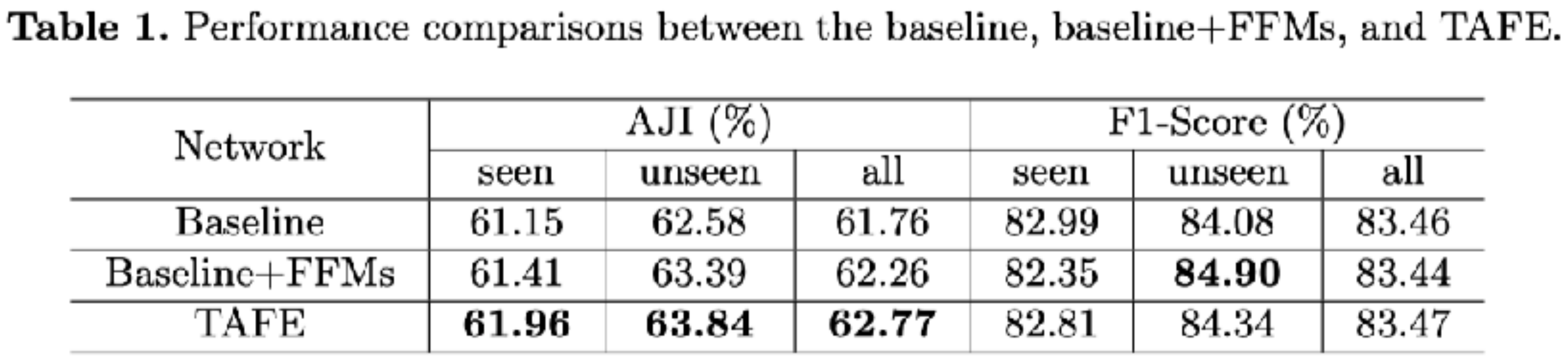

Table 1. Performance comparisons between the baseline, baseline+FFMs, and TAFE.

Network	AJI (%)			F1-Score (%)		
	seen	unseen	all	seen	unseen	all
Baseline	61.15	62.58	61.76	82.99	84.08	83.46
Baseline+FFMs	61.41	63.39	62.26	82.35	**84.90**	83.44
TAFE	**61.96**	**63.84**	**62.77**	82.81	84.34	83.47

Results:

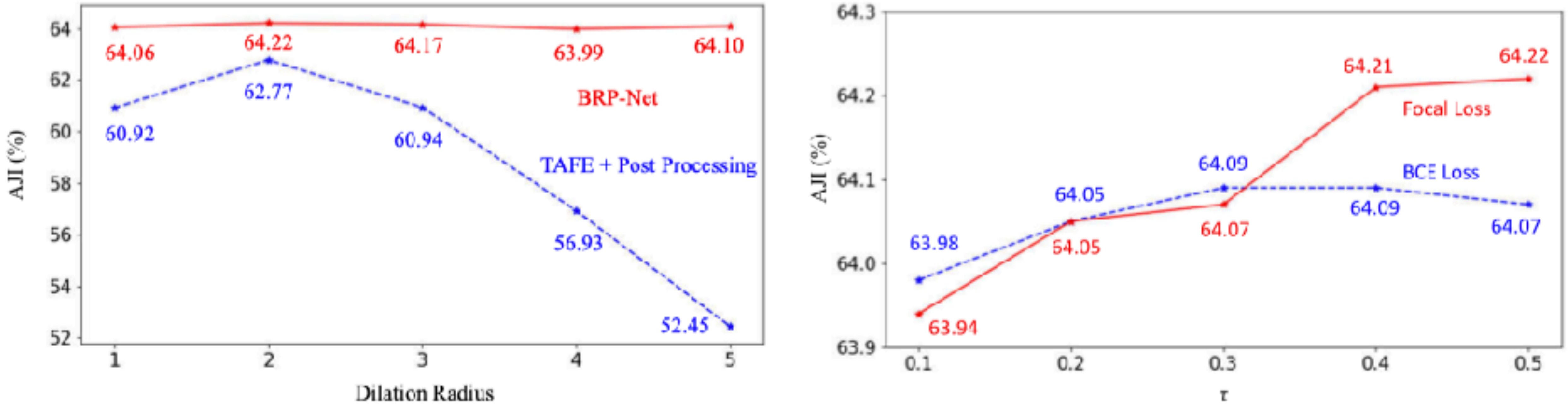

(a)

(b)

Fig. 5. Evaluation on different settings for BRP-Net. (a) The influence of different dilation radii in the post-processing step of TAFE. (b) The choice of IoU thresholds τ and different loss functions for the second stage of BRP-Net.

Results:

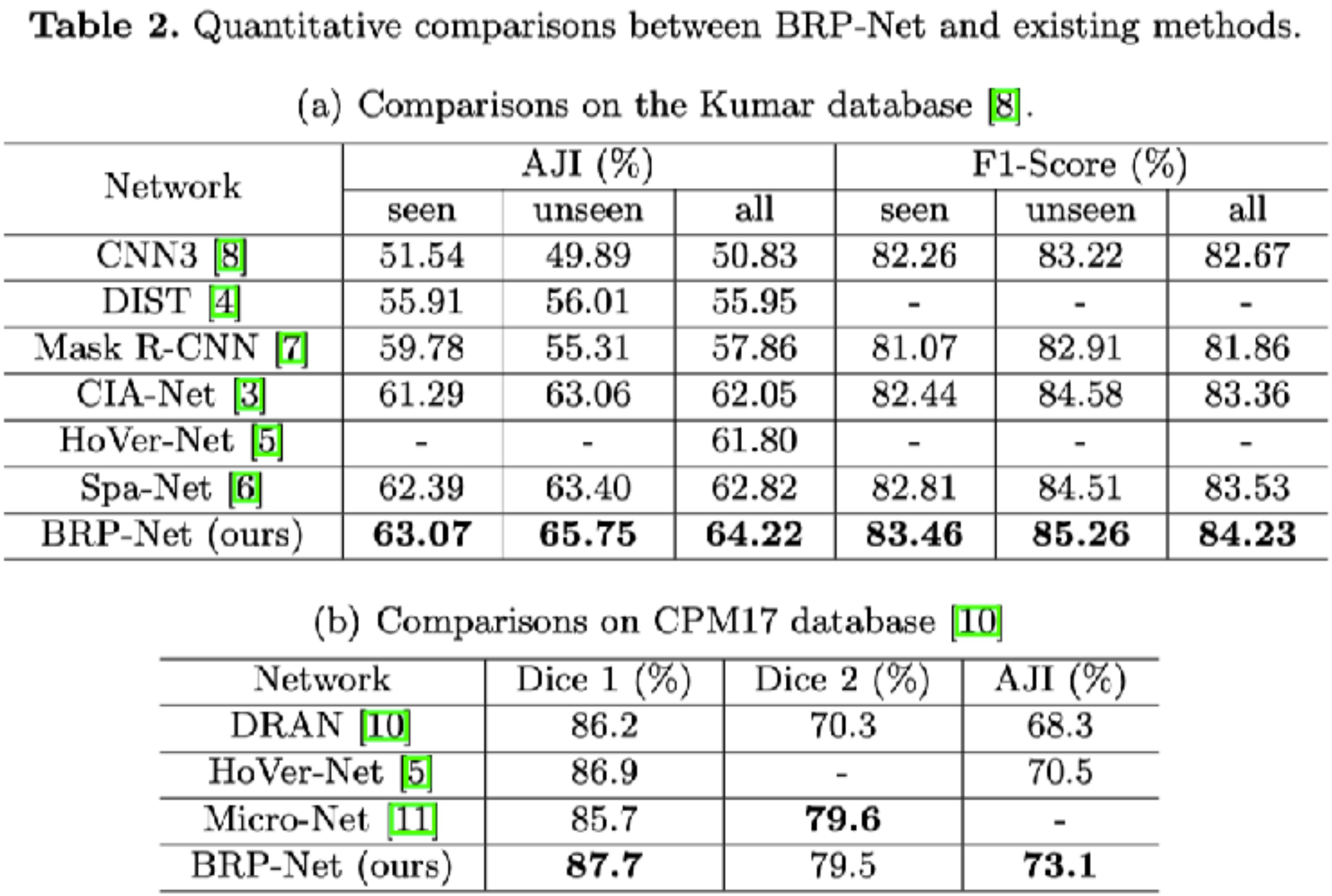

Table 2. Quantitative comparisons between BRP-Net and existing methods.

(a) Comparisons on the Kumar database [8].

Network	AJI (%)			F1-Score (%)		
	seen	unseen	all	seen	unseen	all
CNN3 [8]	51.54	49.89	50.83	82.26	83.22	82.67
DIST [4]	55.91	56.01	55.95	-	-	-
Mask R-CNN [7]	59.78	55.31	57.86	81.07	82.91	81.86
CIA-Net [3]	61.29	63.06	62.05	82.44	84.58	83.36
HoVer-Net [5]	-	-	61.80	-	-	-
Spa-Net [6]	62.39	63.40	62.82	82.81	84.51	83.53
BRP-Net (ours)	**63.07**	**65.75**	**64.22**	**83.46**	**85.26**	**84.23**

(b) Comparisons on CPM17 database [10]

Network	Dice 1 (%)	Dice 2 (%)	AJI (%)
DRAN [10]	86.2	70.3	68.3
HoVer-Net [5]	86.9	-	70.5
Micro-Net [11]	85.7	**79.6**	-
BRP-Net (ours)	**87.7**	79.5	**73.1**

Cell R-CNN V3: A Novel Panoptic Paradigm for Instance Segmentation in Biomedical Images

Dongnan Liu, Donghao Zhang, Yang Song, Member, IEEE, Heng Huang, and Weidong Cai, Member, IEEE

Model:

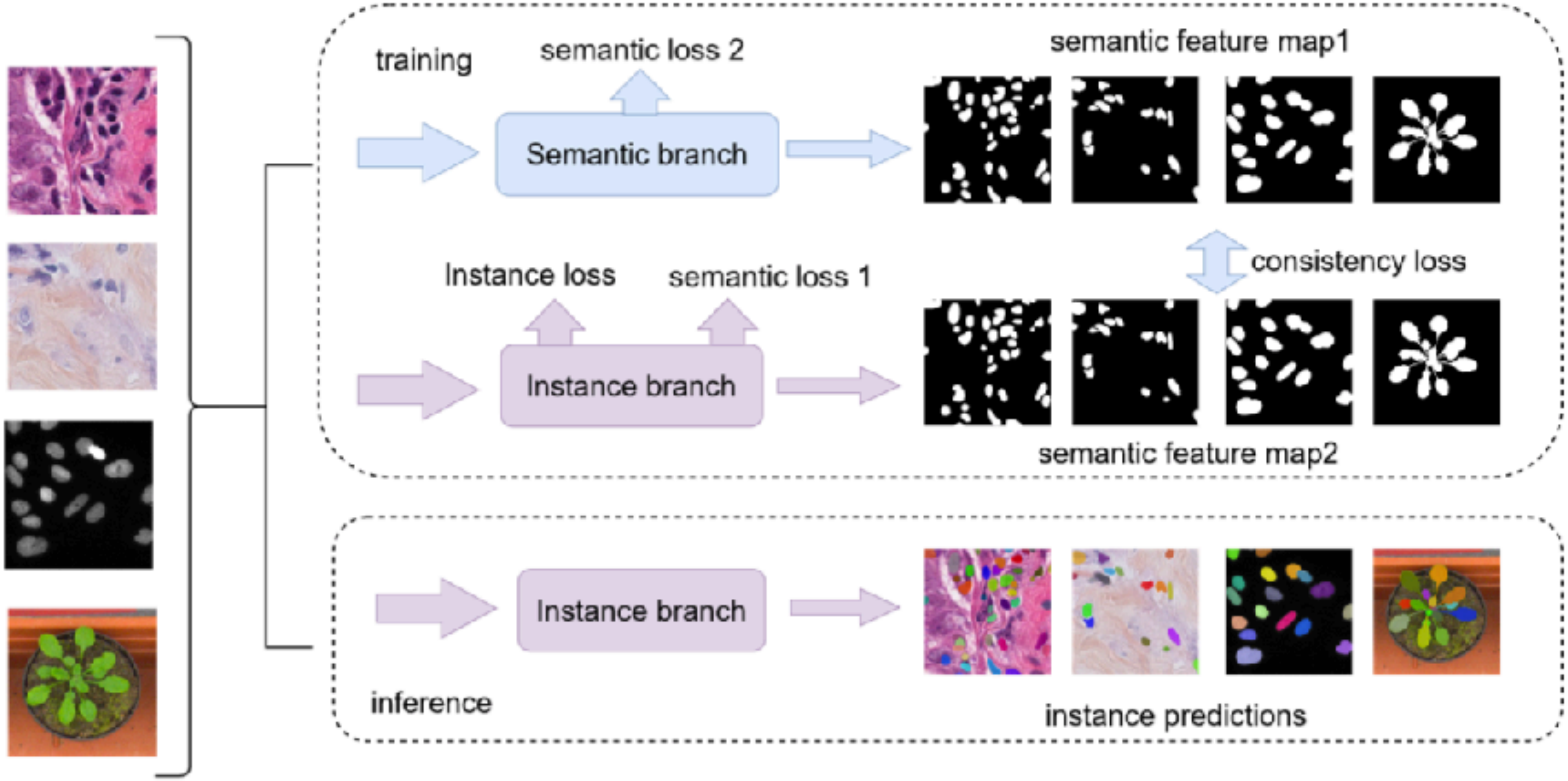
training
semantic loss 2
Semantic branch
semantic feature map1
consistency loss
Instance loss
semantic loss 1
Instance branch
semantic feature map2
Instance branch
inference
instance predictions

Model:

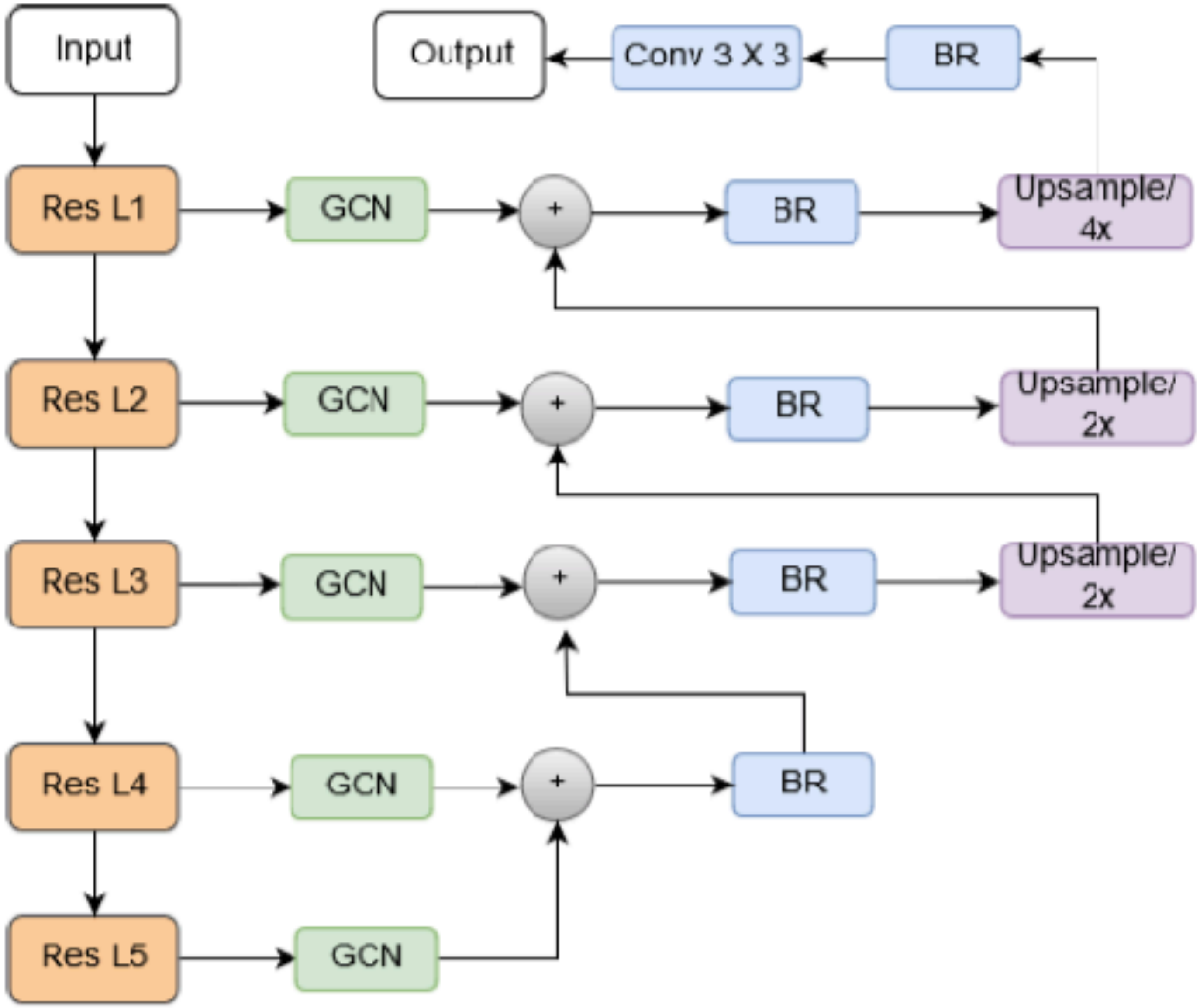

Semantic branch

Model:

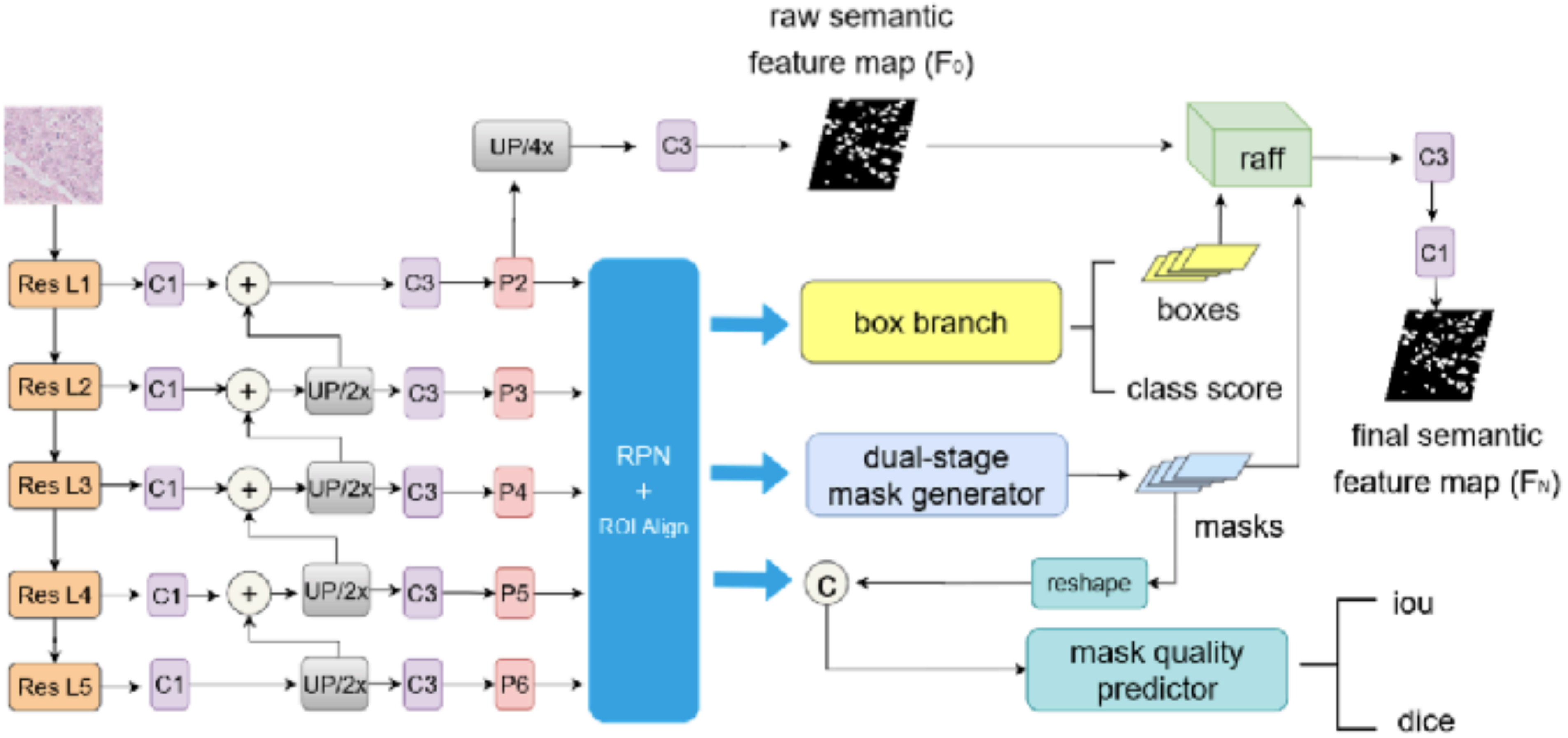

Fig. 2. Overview of our instance segmentation branch. $C1$ and $C3$ represent the convolutional layer with the kernel size of 1 and 3 respectively. The C before the mask quality predictor is the concatenation operation. UP/nx means the upsampling layer for n times with the nearest interpolation. $raff$ represents the proposed residual attention feature fusion mechanism. The ReLU and group normalization layer after all the convolutional layers are omitted for brevity.

Residual attention feature fusion mechanism + Mask quality branch

Model:

Residual attention feature fusion mechanism

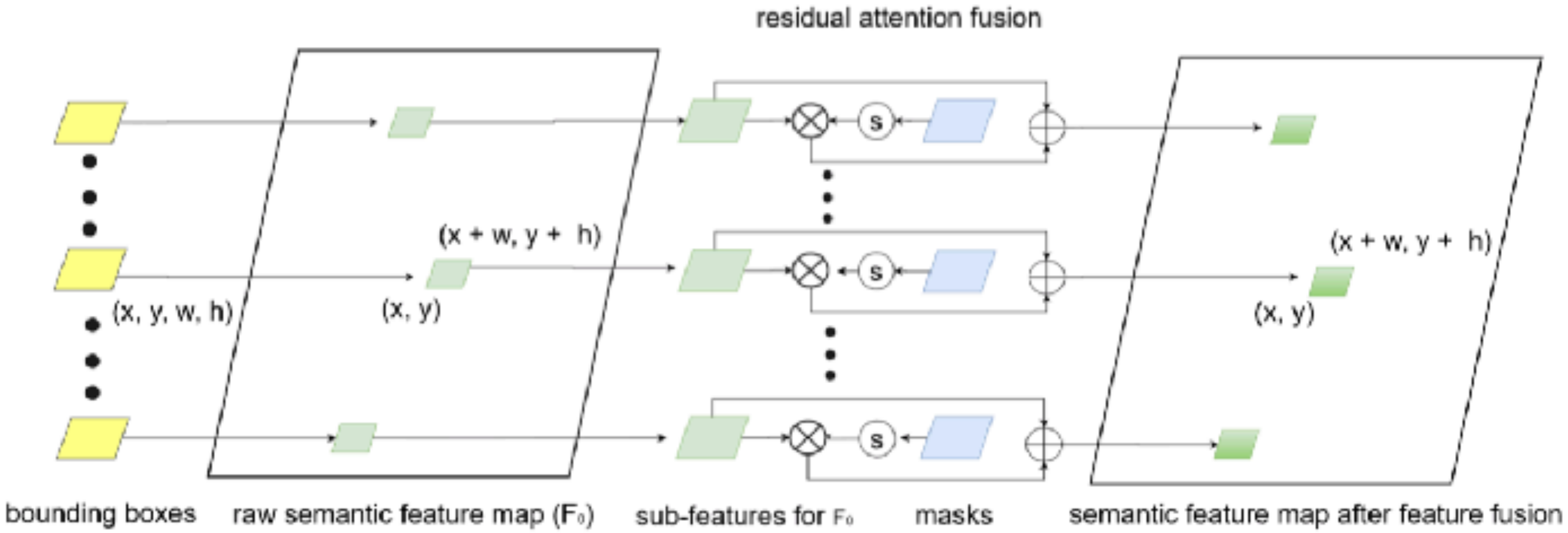
residual attention fusion
(x + w, y + h)
(x, y, w, h)
(x, y)
S
(x + w, y + h)
(x, y)
bounding boxes
raw semantic feature map (F₀)
sub-features for F₀
masks
semantic feature map after feature fusion

Fig. 4. The proposed residual attention feature fusion mechanism. S is the sigmoid operation, $\times$ is the element-wise multiplication, and $+$ is the element-wise summation.

Model:

Mask quality branch (Mask scoring R-CNN(CVPR 2019 oral))

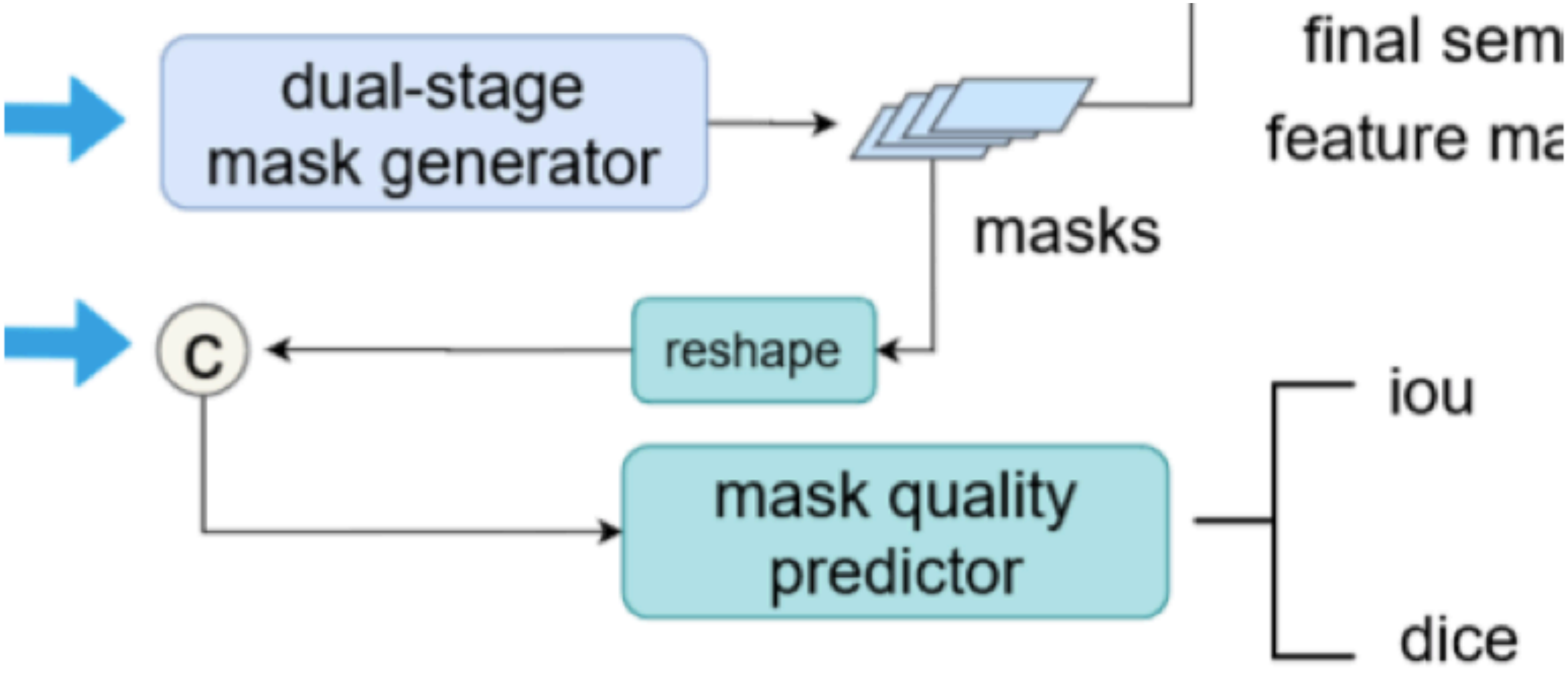

Results:

Datasets: TCGA-Kumar

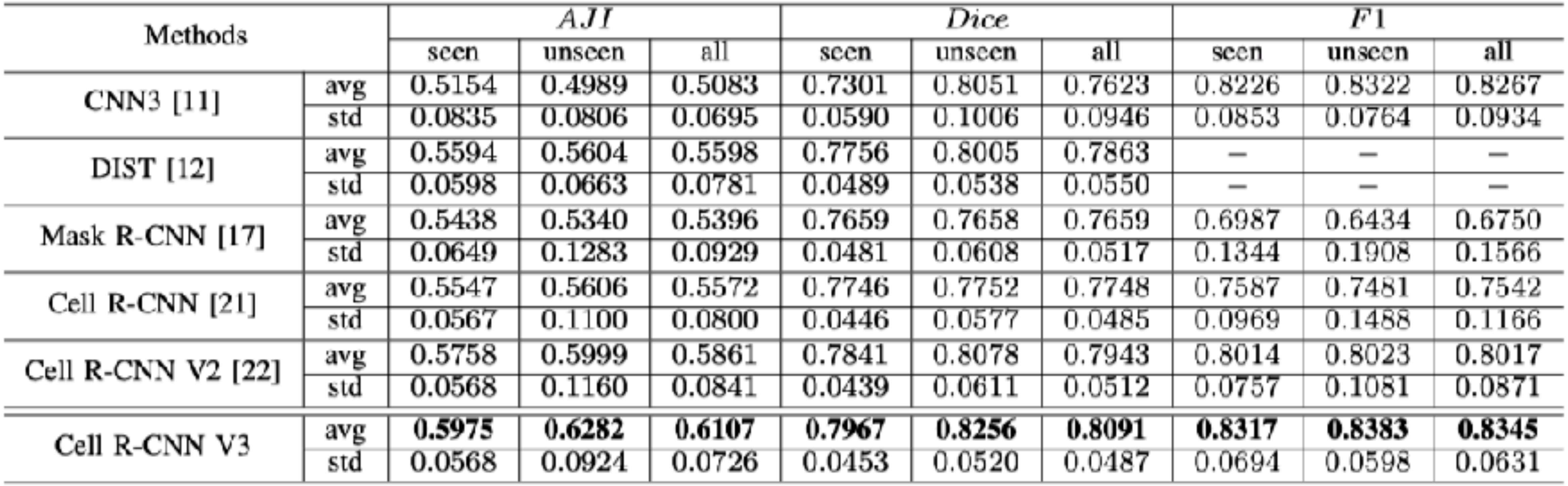

Methods		AJI			$Dice$			$F1$		
		seen	unseen	all	seen	unseen	all	seen	unseen	all
CNN3 [11]	avg	0.5154	0.4989	0.5083	0.7301	0.8051	0.7623	0.8226	0.8322	0.8267
	std	0.0835	0.0806	0.0695	0.0590	0.1006	0.0946	0.0853	0.0764	0.0934
DIST [12]	avg	0.5594	0.5604	0.5598	0.7756	0.8005	0.7863	–	–	–
	std	0.0598	0.0663	0.0781	0.0489	0.0538	0.0550	–	–	–
Mask R-CNN [17]	avg	0.5438	0.5340	0.5396	0.7659	0.7658	0.7659	0.6987	0.6434	0.6750
	std	0.0649	0.1283	0.0929	0.0481	0.0608	0.0517	0.1344	0.1908	0.1566
Cell R-CNN [21]	avg	0.5547	0.5606	0.5572	0.7746	0.7752	0.7748	0.7587	0.7481	0.7542
	std	0.0567	0.1100	0.0800	0.0446	0.0577	0.0485	0.0969	0.1488	0.1166
Cell R-CNN V2 [22]	avg	0.5758	0.5999	0.5861	0.7841	0.8078	0.7943	0.8014	0.8023	0.8017
	std	0.0568	0.1160	0.0841	0.0439	0.0611	0.0512	0.0757	0.1081	0.0871
Cell R-CNN V3	avg	**0.5975**	**0.6282**	**0.6107**	**0.7967**	**0.8256**	**0.8091**	**0.8317**	**0.8383**	**0.8345**
	std	0.0568	0.0924	0.0726	0.0453	0.0520	0.0487	0.0694	0.0598	0.0631